

## A tension stiffening model for analysis of RC flexural members under service load

K.A. Patel<sup>1a</sup>, Sandeep Chaudhary<sup>\*2</sup> and A.K. Nagpal<sup>1b</sup>

<sup>1</sup>Civil Engineering Department, Indian Institute of Technology Delhi, New Delhi 110016, India

<sup>2</sup>Civil Engineering Department, Malaviya National Institute of Technology Jaipur, Jaipur 302017, India

(Received February 13, 2015, Revised December 17, 2015, Accepted December 24, 2015)

**Abstract.** Tension-stiffening is the contribution of concrete between the cracks to carry tensile stresses after cracking in Reinforced Concrete (RC) members. In this paper, a tension-stiffening model has been proposed for computationally efficient nonlinear analysis of RC flexural members subjected to service load. The proposed model has been embedded in a typical cracked span length beam element. The element is visualized to consist of at the most five zones (cracked or uncracked). Closed form expressions for flexibility and stiffness coefficients and end displacements have been obtained for the cracked span length beam element. Further, for use in everyday design, a hybrid analytical-numerical procedure has been developed for nonlinear analysis of RC flexural members using the proposed tension-stiffening model. The procedure yields deflections as well as redistributed bending moments. The proposed model (and developed procedure) has been validated by the comparison with experimental results reported elsewhere and also by comparison with the Finite Element Method (FEM) results. The procedure would lead to drastic reduction in computational time in case of large RC structures.

**Keywords:** cracking; finite element method; reinforced concrete; service load; tension stiffening

### 1. Introduction

Reinforced Concrete (RC) flexural members are widely used in building and bridge construction. At service load, cracking may occur in a zone of a member where the stress at tensile face exceeds the tensile strength of concrete. For example, in a RC continuous member, cracking may occur within the span and near the supports as shown in Fig. 1. In a cracked zone of a RC flexural member, the concrete between the cracks carries tensile stresses owing to bond between steel bars and concrete and this phenomenon is known as tension stiffening. The tension-stiffening effect mainly depends on reinforcement content, type/nature of loadings, member dimensions, number of steel bar layers etc.

The cracking may result in an increase in deflections, considerable moment redistribution along

---

\*Corresponding author, Ph. D., E-mail: [schaudhary.ce@mnit.ac.in](mailto:schaudhary.ce@mnit.ac.in); [sandeep.nitjaipur@gmail.com](mailto:sandeep.nitjaipur@gmail.com)

<sup>a</sup> Ph. D. Student, E-mail: [iitd.kashyap@gmail.com](mailto:iitd.kashyap@gmail.com)

<sup>c</sup> Ph. D., E-mail: [aknagpal@civil.iitd.ac.in](mailto:aknagpal@civil.iitd.ac.in)

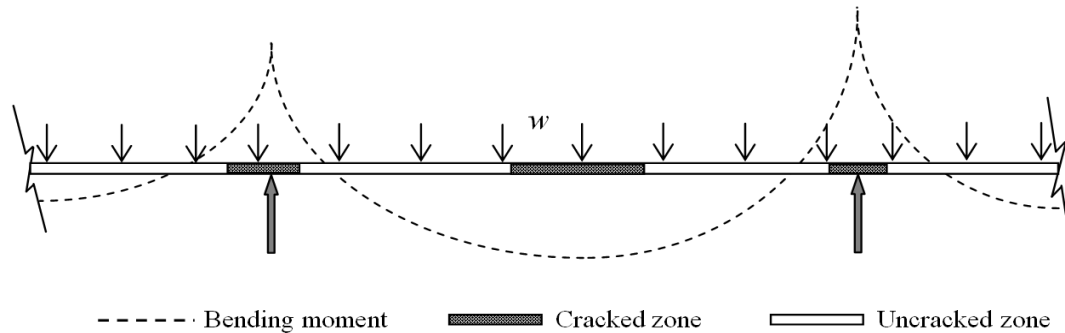


Fig. 1 A typical intermediate span of a RC member with loads, bending moment, and possible cracked-uncracked zones

the member length, and stress redistribution across the cross-sections. The tension-stiffening has significant influence on the deflections, moment redistribution and stress redistribution (Sahamitmongkol and Kishi 2011, Parrotta *et al.* 2014). The appropriate tension-stiffening model for nonlinear analysis of RC structures subjected to service load is therefore important for accurate evaluation of cracking.

A large number of tension-stiffening models are available in the literature for the analysis of RC structures considering concrete cracking. These models may be categorized in two types: Type A and Type B. Type A models are those which discretize the members into a number of elements along length and across the cross-section and Type B models are those in which use is made of effective moment of inertia and the transformed section properties of members.

Type A models can be further subdivided in two categories: Category 1 (macroscopic models) and Category 2 (microscopic models). First, consider category 1 or macroscopic models. In these models, the constitutive (average stress-strain) equation of steel or concrete is modified to account for tension stiffening effect. Some researchers (Smadi and Belakhdar 2007, Salys *et al.* 2009) have modified the constitutive equation for steel, whereas others (Balakrishnan and Murray 1988, Massicote *et al.* 1990) have modified the constitutive equation for concrete. Next, consider Category 2 or microscopic models. In these models, bond-slip relationships is proposed at the interface of concrete and steel bar in a cracked zone using fracture mechanics principles (Lackner and Mang 2003, Borosnyói and Balázs 2005, Ruiz *et al.* 2007, Vollum *et al.* 2008, Shayanfar and Safiey 2008, Dai *et al.* 2012). The microscopic models are complex than the macroscopic models (Stramandinoli and Rovere 2008). Both category 1 and 2 tension-stiffening models of Type A are accurate but require too large computational effort owing to discretization of members into number of elements. The models are therefore not appropriate for use by everyday design engineers.

Now, consider Type B models. As stated earlier, these models are generally based on effective moment of inertia and the transformed section properties of members. Cosenza (1990) used different such tension stiffening models for the analysis of RC beams. Ning *et al.* (1999) proposed probability based effective stiffness model to take into account cracking and tension-stiffening. These models are appropriate for use in everyday design since the required computational effort is small. However, a constant value of moment of inertia (same moment-curvature relationship) is assumed along the member lengths in Type B models. This assumption can lead to errors in case of common types of construction: slab-beam construction of a RC structure. The middle portion (where sagging moment occurs) and at the ends (where hogging moment occurs) of a beam would

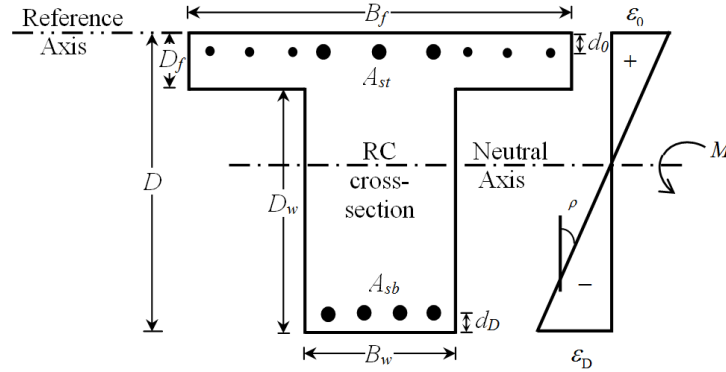


Fig. 2 Typical cross-section of a RC member and strain distribution

have different cross-section (rectangular or T) depending on whether the neutral axis lies within or outside the flange (Patel *et al.* 2014).

In codes of practice (ACI 318 2005, CEN-Eurocode 2 2004), simplified expressions (based on Type B models) are available for estimation of deflections in flexural members. However, these expressions are not appropriate since under-estimation of deflections for lightly reinforced members has been reported (Ghali 1993, Scanlon *et al.* 2001, Bischoff 2005, Gilbert 2006, Patel *et al.* 2015). Further, no expressions for redistributed moments, resulting from cracking and tension-stiffening effect, are available (Patel *et al.* 2014). Therefore, for application to large RC structures, a computationally efficient tension-stiffening model is desired to be developed.

Herein, a tension-stiffening model has been proposed and a hybrid procedure has been developed for nonlinear analysis of RC flexural members (one-way slabs, beams and bridges) taking into account cracking of concrete. Using the proposed tension stiffening model, a typical span length flexural member is considered as a single element and is visualized to consist of at the most five zones (cracked or uncracked). The element is therefore designated as cracked span length beam element. The average interpolation coefficients have been further obtained for cracked zones to keep the procedure analytical at the element level. Closed form expressions for flexibility and stiffness coefficients and end displacements have been obtained for the cracked span length beam element. The proposed model (and developed procedure) has been validated by comparison with experimental results reported elsewhere and also by comparison with Finite Element Method (FEM) results. The hybrid procedure yields deflections as well as redistributed moments. The procedure requires a computational effort which is a fraction of that required in the procedures employing Type A models.

## 2. Cross-sectional analysis

Fig. 2 shows a typical cross-section of a RC member along with the strain distribution. Following assumptions are made for the cross-sectional analysis:

- (i) It is assumed that plane cross-section remains plane after the bending of the member.
- (ii) It is also assumed that there is no slip at the interface of the steel reinforcement and concrete.
- (iii) Before cracking of concrete, under service load, the stress-strain relationship of concrete is

assumed to be linear in both compression and tension.

(iv) The concrete portion between the neutral axis and tensile face, across the cross-section, is assumed to be completely cracked, when the stress at tensile face exceeds the tensile strength of concrete,  $f_t$ .

(v) A linear stress-strain relationship is assumed for steel in both tension and compression and the stresses are assumed to be below the yield stress.

The curvature  $\rho$ , strain  $\varepsilon_y$  at a distance  $y$  from the reference axis, strain at reference axis  $\varepsilon_0$ , and stress at reference axis  $\sigma_0$  due to applied bending moment  $M$ , and axial force  $N$  at a cross-section (see Fig. 2) are given as

$$\rho = \rho^m + \rho^n \quad (1)$$

$$\varepsilon_y = \varepsilon_0 - y\rho \quad (2)$$

$$\varepsilon_0 = \varepsilon_0^m + \varepsilon_0^n \quad (3)$$

$$\sigma_0 = E_c \varepsilon_0 \quad (4)$$

where,

$$\rho^m = S^x M \quad (5)$$

$$\rho^n = S^{xy} N \quad (6)$$

$$\varepsilon_0^m = S^{yx} M \quad (7)$$

$$\varepsilon_0^n = S^y N \quad (8)$$

where, the superscripts,  $m$ ,  $n$  here and subsequently in other quantities indicate that the quantity corresponds to moment  $M$ , and axial force  $N$ , respectively. In Eqs. (5) and (7), the moment  $M$  at a section in the counter clockwise direction on the face with normal in the positive X-axis is taken as positive. The quantities  $S^x$ ,  $S^{xy}$ ,  $S^{yx}$ ,  $S^y$  are given as

$$S^x = \frac{A}{E_c (AI - B^2)} \quad (9)$$

$$S^{xy} = S^{yx} = \frac{B}{E_c (AI - B^2)} \quad (10)$$

$$S^y = \frac{I}{E_c (AI - B^2)} \quad (11)$$

where  $E_c$  = modulus of elasticity of concrete at 28 days;  $A$  = area of the transformed cross-section; and  $B$ ,  $I$  = first and second moment of area of the transformed cross-section about the reference axis respectively. The reference axis for the cross-section is assumed to be at the top fiber since the location of neutral axis varies for the cracked and uncracked cross-section along the member.

Assuming that there is no axial force in continuous members,  $\rho$  and  $\varepsilon_0$  are given as

$$\rho = S^x M \tag{12}$$

$$\varepsilon_0 = S^{xy} M \tag{13}$$

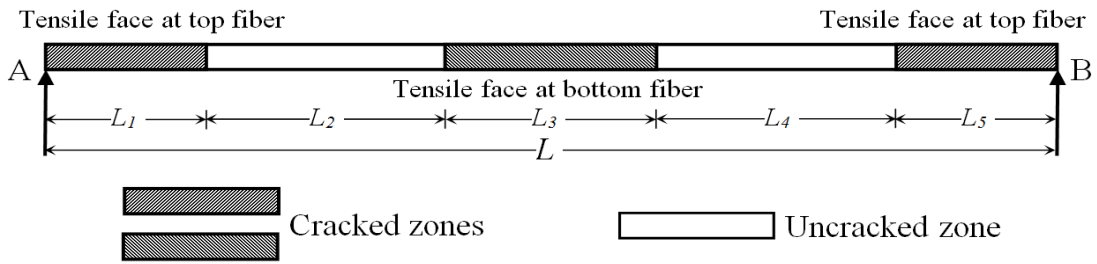


Fig. 3 Possible zones, cracked or uncracked, in a typical span of a member

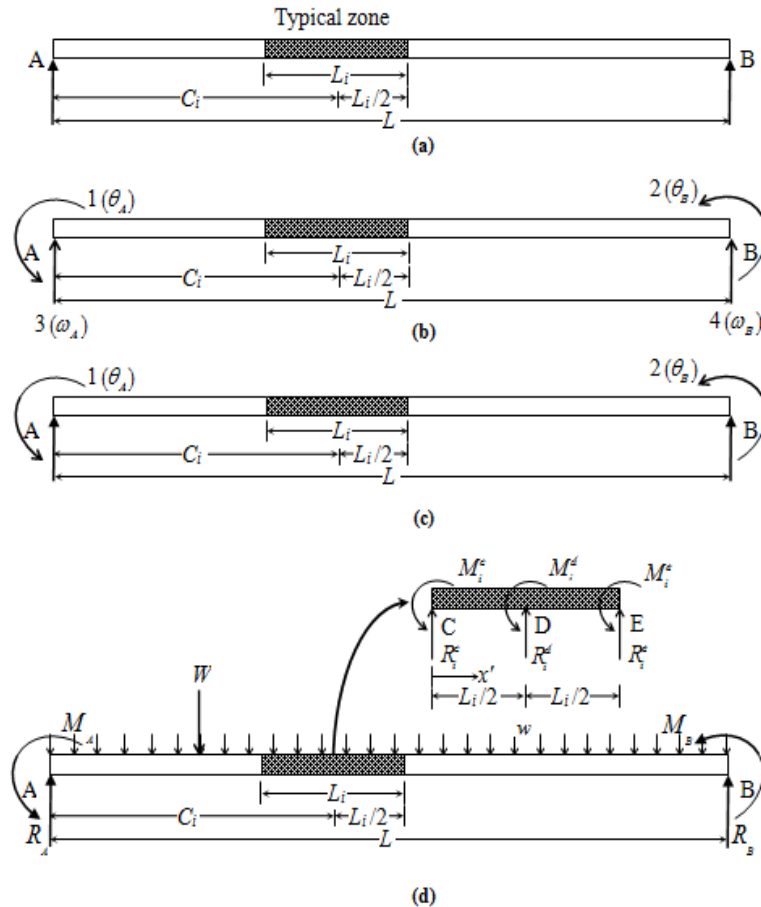


Fig. 4 A span length beam element (a) typical zones (cracked or uncracked); (b) degrees of freedom; (c) releases; and (d) loads and end forces

### 3. Cracked span length beam element

In a typical intermediate span of a continuous member, cracking may occur at the middle portion and at the ends if the tensile stress at bottom fiber or top fiber of a cross-section exceeds the tensile strength of concrete respectively. Fig. 3 shows possible zones, cracked or uncracked, in a typical intermediate span of a continuous member. There may be maximum five zones in a span, three cracked zones (one at in-span and two at ends) and two uncracked zones between the cracked zones. Fig. 4(a) shows the position of a typical zone of length,  $L_i$  (cracked or uncracked) in a span of a member. The entire span is modeled as a single element and is therefore designated as a cracked span length beam element.

#### 3.1 Tension stiffening model

First, consider a cross-section in the cracked zone. The tension stiffening effect is taken into account by considering the cross-section in two states, uncracked and cracked. The properties of the cross-section incorporating tension stiffening are arrived at by suitably combining the uncracked and cracked cross-section properties. The transformed properties  $A, B, I$  of cross-section in cracked state are obtained by neglecting the concrete between the neutral axis and tensile face and taking moments of area about the reference axis.

The curvature,  $\rho_{ts}$  and the top fiber strain,  $\varepsilon_{0,ts}$  of a cross-section in a cracked zone (the subscript,  $ts$  here and subsequently in other quantities indicates that the tension stiffening effect has been taken into account) are equal to  $\eta\rho_{un} + \zeta\rho_{cr}$  and  $\eta\varepsilon_{0,un} + \zeta\varepsilon_{0,cr}$  respectively (the subscripts,  $un$  and  $cr$  here and subsequently in other quantities indicate that the quantities are evaluated using uncracked and cracked cross-sectional properties respectively), where,  $\zeta\eta$  = interpolation coefficients, which are defined as (Ghali 1993)

$$\zeta = 1 - \eta = 1 - (\kappa f_t / \sigma_{un})^2 \quad (14)$$

where,  $\kappa$  = coefficient representing influence of duration of application or repetition of loading; 0.8 for initial/first loading and 0.5 for long-term loading or for a large number of load cycles and  $\sigma_{un}$  = stress at tensile face. The interpolation coefficients  $\zeta, \eta$  are dimensionless and they represent the extent of cracking. At the start of cracking,  $\zeta=0$  and its value tends to 1 (corresponding  $\eta$  tends to 0) with increasing applied stresses (Ghali *et al.* 2002).

Next, consider a cross-section in the uncracked zone. The curvature,  $\rho_{un}$  and the top fiber strain,  $\varepsilon_{0,un}$  in this zone are equal to their respective values in the uncracked state only ( $\zeta=0$  and  $\eta=1$ ).

In order to take into account tension stiffening effect without discretising the member, an average interpolation coefficient,  $\zeta$  is considered for each cracked zone. For this purpose first, average stresses,  $\sigma_{t,un,i}$ ,  $\sigma_{b,un,i}$  for cracked zones are obtained as

$$\sigma_{t,un,i} = \frac{1}{L_{i,cr}} \int_{-\frac{L_{i,cr}}{2}}^{\frac{L_{i,cr}}{2}} \sigma_{t,un} dx \quad (15)$$

$$\sigma_{b,un,i} = \frac{1}{L_{i,cr}} \int_{-\frac{L_{i,cr}}{2}}^{\frac{L_{i,cr}}{2}} \sigma_{b,un} dx \quad (16)$$

where,  $\sigma_{t,un}$ ,  $\sigma_{b,un}$ = stresses at tensile face (at top fiber and at bottom fiber respectively), and  $L_{i,cr}$ = length of the cracked zone.

The average interpolation coefficient,  $\zeta_i$  for the all cracked zones are then evaluated from Eq. (14) on replacing  $\sigma_{un}$  by either  $\sigma_{t,un,i}$  or  $\sigma_{b,un,i}$ . Further, in case of initial/first loading, for a concentrated load, the value of  $\kappa$  (in Eq. (14)) is recommended as 0.55, since  $\sigma_{un}$  is farther away from  $\sigma_{t,un,i}$  or  $\sigma_{b,un,i}$  than for other loadings such as uniformly distributed load or two point loading for which as stated earlier, the value of  $\kappa$  is 0.80.

### 3.2 Shear deformation model

The effect of shear deformation can be significant for a member with small span/depth ratio. The shearing rigidity  $K$  of uncracked section,  $K_{un}$  and of cracked section,  $K_{cr}$  are given as (Park and Paulay 1975)

$$K_{un} = \frac{GB_w d}{f} \tag{17}$$

$$K_{cr} = \frac{\nu_v E_s B_w d}{1 + 4n\nu_v} \tag{18}$$

where, shear modulus of concrete,  $G=E_c/2(1+\mu)$ ; modular ratio,  $n=E_s/E_c$ ;  $E_s$ =modulus of elasticity of steel;  $\mu$  = Poisson’s ratio of concrete;  $B_w$ =width of web;  $d$ =effective depth of section;  $f$ =shear coefficient (taken as 1.2 for rectangular section and 1.0 for T section); shearing steel content  $\nu_v=A_v/sB$ ;  $A_v$ = shearing steel area;  $s$ = spacing of reinforcements.

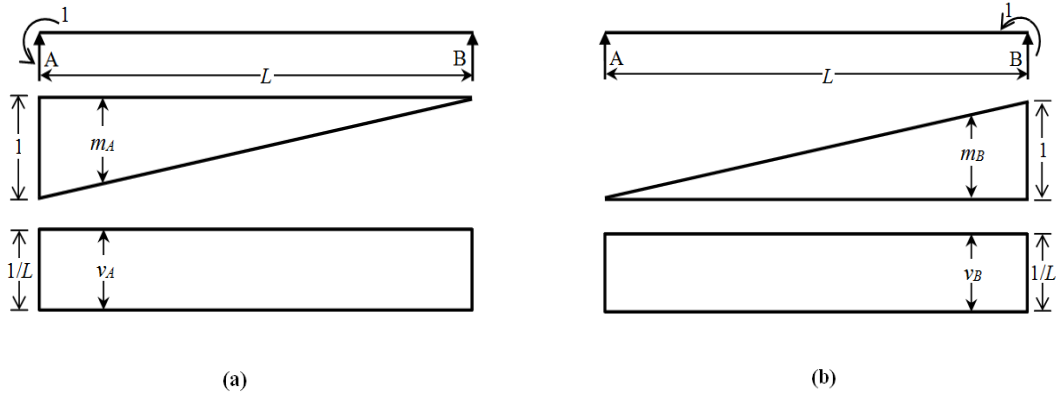


Fig. 5 (a)  $m_A$  (bending moment),  $v_A$  ( $=m_A/L$ , shear force); and (b)  $m_B$  (bending moment),  $v_B$  ( $=m_B/L$ , shear force) diagrams

### 3.3 Stiffness matrix

The stiffness matrix,  $[k]$  of a cracked span length beam element with four degrees of freedom (see Fig. 4(b)) is of interest. First, consider an element with releases 1, 2 corresponding to degrees

of freedom 1, 2 introduced at the ends (of released span length beam element) as shown in Fig. 4(c). The flexibility matrix coefficients corresponding to these releases are derived by the principle of virtual work using  $m_A$  (bending moment),  $v_A$  ( $=m_A/L$ , shear force),  $m_B$  (bending moment) and  $v_B$  ( $=m_B/L$ , shear force) diagrams (see Fig. 5), which are obtained by applying unit forces corresponding to releases 1 and 2 respectively, as

$$f_{11} = \int_0^L \left( S^x m_A^2 + \frac{v_A^2}{K} \right) dx \quad (19)$$

$$f_{12} = f_{21} = \int_0^L \left( S^x m_A m_B + \frac{v_A v_B}{K} \right) dx \quad (20)$$

$$f_{22} = \int_0^L \left( S^x m_B^2 + \frac{v_B^2}{K} \right) dx \quad (21)$$

Eqs. (19)-(21) are to be integrated for a cracked span length beam element. For a cross-section in a typical zone, considering the tension stiffening effect,  $S^x$  is to be replaced by  $\zeta_i S_{cr,i}^x + \eta_i S_{un}^x$ .

The closed form expressions for flexibility matrix coefficients of a cracked span length beam element, assuming constant transformed cross-section properties in a typical zone are obtained as

$$f_{11} = \frac{1}{12L^2} \sum_{i=1}^5 (\zeta_i S_{cr,i}^x + \eta_i S_{un}^x) (12L^2 L_i - 24C_i L L_i + L_i^3 + 12C_i^2 L_i) + \frac{1}{KL} \quad (22)$$

$$f_{12} = f_{21} = \frac{1}{12L^2} \sum_{i=1}^5 (\zeta_i S_{cr,i}^x + \eta_i S_{un}^x) (L_i^3 + 12C_i^2 L_i - 12C_i L L_i) - \frac{1}{KL} \quad (23)$$

$$f_{22} = \frac{1}{12L^2} \sum_{i=1}^5 (\zeta_i S_{cr,i}^x + \eta_i S_{un}^x) (L_i^3 + 12C_i^2 L_i) + \frac{1}{KL} \quad (24)$$

where,  $L$ =length of the span;  $L_i$ =length of the typical zone,  $C_i$ =distance from end A to center of the typical zone.

The coefficients of stiffness matrix,  $[k]$  corresponding to degrees of freedom 1, 2 are now obtained by inverting the flexibility matrix coefficients corresponding to degrees of freedom 1, 2 (on using the readily available expressions for inversion of  $2 \times 2$  matrix). Remaining terms corresponding to degrees of freedom 3, 4 are obtained by applying the equilibrium conditions (Ghali *et al.* 2002, 2003) and the stiffness matrix,  $[k]$  corresponding to all degrees of freedom (1 to 4) is obtained as

$$[k] = \begin{matrix} & \begin{matrix} 1 & 2 & 3 & 4 \end{matrix} \\ \begin{matrix} 1 \\ 2 \\ 3 \\ 4 \end{matrix} & \begin{bmatrix} k_{11} & k_{12} & (k_{11} + k_{12})/L & -(k_{11} + k_{12})/L \\ k_{21} & k_{22} & (k_{21} + k_{22})/L & -(k_{21} + k_{22})/L \\ (k_{11} + k_{12})/L & (k_{21} + k_{22})/L & (k_{11} + k_{12} + k_{21} + k_{22})/L & -(k_{11} + k_{12} + k_{21} + k_{22})/L \\ -(k_{11} + k_{12})/L & -(k_{21} + k_{22})/L & -(k_{11} + k_{12} + k_{21} + k_{22})/L & (k_{11} + k_{12} + k_{21} + k_{22})/L^2 \end{bmatrix} \end{matrix} \quad (25)$$

where,  $k_{11}=f_{22}/(f_{11}f_{22}-f_{12}f_{21})$ ;  $k_{12}=k_{21}=-f_{12}/(f_{11}f_{22}-f_{12}f_{21})$ ;  $k_{22}=f_{11}/(f_{11}f_{22}-f_{12}f_{21})$ .

### 3.4 End rotations and deflection

Now, consider the end displacements of the released span length beam element subjected to loads, end moments and forces (see Fig. 4(d)). For this purpose, first, the moment  $M_i(x')$  and shear force  $R_i(x')$  in a typical zone may be obtained, assuming the moment, and shear force variation to be parabolic (see Fig. 4(d)), as

$$M_i(x') = \frac{1}{L_i^2} \left[ (2x' - L_i)(x' - L_i)M_i^c - 4x'(x' - L_i)M_i^d + x'(2x' - L_i)M_i^e \right] \quad (26)$$

$$R_i(x') = \frac{1}{L_i} \left[ (2x' - L_i)(x' - L_i)R_i^c - 4x'(x' - L_i)R_i^d + x'(2x' - L_i)R_i^e \right] \quad (27)$$

where,  $M_i^c, M_i^d, M_i^e$  = the moment at C, D, E, respectively,  $R_i^c, R_i^d, R_i^e$  = the shear force at C, D, E, respectively and  $x'$  = distance of cross-section from C in a typical zone (see Fig. 4(d)).

The rotation  $\theta_A$  may be expressed in closed form as summation of integration of  $m_A$  (bending moment) diagram and  $v_A$  ( $=m_A/L$ , shear force) diagram with  $\rho(x)$  and  $(R_i/K)(x)$  respectively. The value of  $\rho$  can be obtained from Eq. (12) on substitution of  $M$  by  $M_i$ . Similarly, the rotation  $\theta_B$  may be obtained using  $m_B$  (bending moment) diagram and  $v_B$  ( $=m_B/L$ , shear force) diagram. The expressions for  $\theta_A$  and  $\theta_B$ , assuming constant transformed cross-section properties in a typical zone are obtained as

$$\theta_A = \frac{1}{L} \sum_{i=1}^5 \left[ \frac{1}{36L_i^2} (\xi_i S_{cr,i}^x + \eta_i S_{un}^x) \left\{ \begin{aligned} &6M_i^q C_i^2 L_i (C_i - L) - 36M_i^r C_i L_i^2 (C_i - L) \\ &+ 6M_i^p L_i^3 (C_i - L) + M_i^q C_i L_i^3 - 3M_i^r L_i^4 \end{aligned} \right\} \right] \\ + \frac{1}{LK} \sum_{i=1}^5 \left[ \frac{1}{6L_i^2} \{ R_i^p L_i^3 + R_i^q C_i^2 L_i - 6R_i^r C_i L_i^2 \} \right] \quad (28)$$

$$\theta_B = \frac{1}{L} \sum_{i=1}^5 \left[ \frac{1}{36L_i^2} (\xi_i S_{cr,i}^x + \eta_i S_{un}^x) \left\{ \begin{aligned} &6M_i^q C_i^3 L_i - 36M_i^r C_i^2 L_i^2 \\ &+ 6M_i^p C_i L_i^3 + M_i^q C_i L_i^3 - 3M_i^r L_i^4 \end{aligned} \right\} \right] \\ - \frac{1}{LK} \sum_{i=1}^5 \left[ \frac{1}{6L_i^2} \{ R_i^p L_i^3 + R_i^q C_i^2 L_i - 6R_i^r C_i L_i^2 \} \right] \quad (29)$$

where,  $M_i^p = 7M_i^c - 2M_i^d + M_i^e$ ;  $M_i^q = 12M_i^c - 24M_i^d + 12M_i^e$ ; and  $M_i^r = 3M_i^c - 4M_i^d + M_i^e$ .

The mid-span deflection,  $d_m$  of a cracked span length beam element subjected to loading and end forces may be expressed as

$$d_m = \frac{1}{2} \left[ \int_0^{L/2} \rho(x) x dx + L \int_{L/2}^L \rho(x) \left( 1 - \frac{x}{L} \right) dx \right] \quad (30)$$

and may be obtained either analytically or numerically.

#### 4. Hybrid analytical-numerical procedure for analysis of RC continuous members

An iterative process is required to establish the zone lengths and stiffness coefficients that is initiated by assuming the entire element to be uncracked. For a typical iterative cycle, a displacement analysis is carried out for the residual force vector,  $\{P^{er}\}$  of the element. The revised force vector  $\{p\}$  ( $\{p\}^T = \{M_A, M_B\}$ ) and the revised displacement vector of the element (see Fig. 4(d)),  $\{d^*\}$  ( $\{d^*\}^T = \{\theta_A^*, \theta_B^*\}$ ) are obtained by adding the force vector and displacement vector evaluated in the present cycle to the force vector and displacement vector at the end of previous cycle respectively.

Based on the revised force vector,  $\{p\}$ , the revised zone (cracked and uncracked) lengths,  $L_i$  of a element are established by locating the cross-sections where either  $\sigma_{t,un}$  or  $\sigma_{b,un}$  is equal to  $-f_t$ . The stresses  $\sigma_{t,un}$ ,  $\sigma_{b,un}$  for a cross-section at a distance  $x$  from end A are obtained from Eq. (4), on substitution of  $M$  by revised  $M_x$  as

$$\sigma_{t,un} = E_c \varepsilon_0 = E_c \left( S_{un}^{xy} M_x \right) \quad (31)$$

$$\sigma_{b,un} = E_c (\varepsilon_0 - D\rho) = E_c \left( (S_{un}^{xy} - DS_{un}^x) M_x \right) \quad (32)$$

Once the revised zone lengths  $L_i$  are established, the revised average interpolation coefficients  $\zeta_i$  are obtained from Eq. (14) on replacing  $\sigma_{un}$  by either  $\sigma_{t,un,i}$  or  $\sigma_{b,un,i}$  (Eqs. (15)-(16)), corresponding to revised cracked zone lengths.

In particular, the closed form expressions of revised cracked zone lengths and corresponding average interpolation coefficients are given below for:

##### 4.1 Concentrated load (see Fig. 6(a))

For evaluating the cracked zone lengths  $L_1$  and  $L_5$  (see Fig. 3), the positions of cross-sections with top fiber stress equal to tensile strength are identified. The parameters,  $\sigma_{t,un}$  and  $M_x$  in Eq. (31) are substituted by  $-f_t$  and  $R_A x - M_A$  (if  $x \leq p$ ) or  $R_A x - M_A - W(x-p)$  (if  $x > p$ ) (where,  $W$ =concentrated load, and  $p$ =distance between concentrated load and end A) respectively to yield

$$-f_t = E_c S_{un}^{xy} \{R_A x - M_A\} \quad (\text{if } x \leq p) \quad (33)$$

$$-f_t = E_c S_{un}^{xy} \{R_A x - M_A - W(x-p)\} \quad (\text{if } x > p) \quad (34)$$

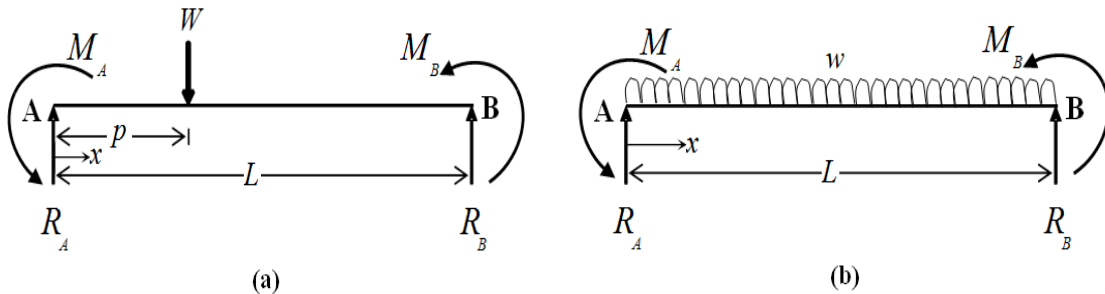


Fig. 6 A typical span of a continuous member with (a) concentrated load; and (b) uniformly distributed load

The cracked zone length  $L_1$  (see Fig. 3) is obtained from Eq. (33) as

$$L_1 = \frac{-b_1}{a_1} \quad (35)$$

where,  $a_1 = S_{un}^{xy} E_c R_A$ ; and  $b_1 = -S_{un}^{xy} E_c M_A + f_t$ .

The length  $L-L_5$  (see Fig. 3) is obtained from Eq. (34) as

$$L - L_5 = -\frac{b_5}{a_5} \quad (36)$$

where,  $a_5 = S_{un}^{xy} E_c (R_A - W)$ ; and  $b_5 = S_{un}^{xy} E_c (Wp - M_A) + f_t$ .

The corresponding average interpolation coefficients,  $\zeta_1$  and  $\zeta_5$  are further obtained from Eqs. (14)-(15) as

$$\zeta_1 = 1 - \kappa \left( \frac{f_t}{a_1 C_1 + b_1 - f_t} \right)^2 \quad (37)$$

$$\zeta_5 = 1 - \kappa \left( \frac{f_t}{a_5 C_5 + b_5 - f_t} \right)^2 \quad (38)$$

where, as stated earlier in section 3.3,  $C_i$  = distance from end A to center of a typical zone of length  $L_i$ .

Now, for evaluating the cracked zone length  $L_3$  (see Fig. 3), the positions of cross-sections with bottom fiber stress equal to tensile strength are identified. The parameters,  $\sigma_{b,un}$  and  $M_x$  in Eq. (32) are substituted by  $-f_t$  and  $R_A x - M_A$  (if  $x \leq p$ ) or  $R_A x - M_A - W(x-p)$  (if  $x > p$ ) (where,  $W$  = concentrated load and  $p$  = distance between concentrated load and end A) respectively to yield

$$-f_t = E_c (S_{un}^{xy} - DS_{un}^x) \{R_A x - M_A\} \quad (\text{if } x \leq p) \quad (39)$$

$$-f_t = E_c (S_{un}^{xy} - DS_{un}^x) \{R_A x - M_A - W(x-p)\} \quad (\text{if } x > p) \quad (40)$$

The length  $L_1 + L_2$ , which defines the left end of cracked zone of length  $L_3$  (see Fig. 3), is obtained from Eq. (39) as

$$L_1 + L_2 = \frac{-b_2}{a_2} \quad (41)$$

where,  $a_2 = E_c R_A (S_{un}^{xy} - DS_{un}^x)$ ; and  $b_2 = -E_c M_A (S_{un}^{xy} - DS_{un}^x) + f_t$ .

The length  $L_1 + L_2 + L_3$  (see Fig. 3), which defines the right end of cracked zone of length  $L_3$ , is obtained from Eq. (40) as

$$L_1 + L_2 + L_3 = \frac{-b_2}{a_2} \quad (42)$$

where,  $a_2 = E_c (S_{un}^{xy} - DS_{un}^x) (R_A - W)$  and  $b_2 = E_c (S_{un}^{xy} - DS_{un}^x) (Wp - M_A) + f_t$ .

The cracked zone length,  $L_3$  is obtained from Eqs. (41)-(42) and the corresponding average

interpolation coefficient,  $\xi_3$  is further obtained from Eqs. (14) and (16) as

$$\xi_3 = 1 - \kappa \left( \frac{f_t}{a_2 C_3 + b_2 - f_t} \right)^2 \quad (43)$$

#### 4.2 Uniformly distributed load (see Fig. 6(b))

For evaluating the cracked zone lengths  $L_1$ ,  $L_5$  (see Fig. 3), the positions of cross-sections with top fiber stress equal to tensile strength are identified. The parameters  $\sigma_{t,un}$  and  $M_x$  in Eq. (31) are substituted by  $-f_t$  and  $R_A x - M_A - wx^2/2$  ( $w$  = uniformly distributed load) respectively to yield

$$-f_t = E_c S^{xy} (R_A x - M_A - wx^2 / 2) \quad (44)$$

The cracked zone lengths,  $L_1$  and  $L_5$  (see Fig. 3) are obtained from Eq. (44) as

$$L_1 = \frac{-b_1 + \sqrt{b_1^2 - 4a_1 c_1}}{2a_1} \quad (45)$$

$$L_5 = L + \frac{b_1 + \sqrt{b_1^2 - 4a_1 c_1}}{2a_1} \quad (46)$$

where,  $a_1 = -0.5 S_{un}^{xy} E_c w$ ;  $b_1 = S_{un}^{xy} E_c R_A$ ; and  $c_1 = -S_{un}^{xy} E_c M_A + f_t$ .

The corresponding average interpolation coefficients  $\zeta_1$ ,  $\zeta_2$  are further obtained from Eqs. (14)-(15) as

$$\xi_1 = 1 - \kappa \left( \frac{12f_t}{a_1(L_1^2 + 12C_1^2) + 12b_1 C_1 + 12(c_1 - f_t)} \right)^2 \quad (47)$$

$$\xi_5 = 1 - \kappa \left( \frac{12f_t}{a_1(L_5^2 + 12C_5^2) + 12b_1 C_5 + 12(c_1 - f_t)} \right)^2 \quad (48)$$

Now, for evaluating the cracked zone length,  $L_3$  (see Fig. 3), the positions of cross-sections with bottom fiber stress equal to tensile strength are identified. The parameters,  $\sigma_{b,un}$  and  $M_x$  in Eq. (32) are substituted by  $-f_t$  and  $R_A x - M_A - wx^2/2$  respectively to yield

$$-f_t = E_c (S^{xy} - DS^x) (R_A x - M_A - wx^2 / 2) \quad (49)$$

The cracked zone length,  $L_3$  (see Fig. 3) is obtained from Eq. (49) as

$$L_3 = \frac{\sqrt{b_3^2 - 4a_3 c_3}}{a_3} \quad (50)$$

where,  $a_3 = -0.5 S_{un}^{xy} E_c w$ ;  $b_3 = (S_{un}^{xy} - DS_{un}^x) E_c R_A$  and  $c_3 = -(S_{un}^{xy} - DS_{un}^x) E_c M_A + f_t$ .

The corresponding average interpolation coefficient  $\zeta_3$  is further obtained from Eqs. (14) and

(16) as

$$\xi_3 = 1 - \kappa \left( \frac{12f_t}{a_2(L_3^2 + 12C_3^2) + 12b_2C_3 + 12(c_2 - f_t)} \right)^2 \quad (51)$$

Revisions in  $L_i$  and corresponding average interpolation coefficient  $\xi_i$  and thereby in end displacements of the element lead to the difference between the displacement vector  $\{d^*\}$ , and the displacement vector evaluated based on integration of curvature and strain. The error (or difference in displacement vector),  $\{d^{er}\}$ , corresponding to releases 1, 2 is now given as

$$\{d^{er}\} = \begin{Bmatrix} \theta_A - \theta_A^* \\ \theta_B - \theta_B^* \end{Bmatrix} \quad (52)$$

where, the rotations  $\theta_A$  and  $\theta_B$  are obtained from Eqs. (28)-(29) respectively. The terms of residual force vector  $\{p^{er}\}$ , of the member, corresponding to this difference in displacement vector are given as  $-[k]\{d^{er}\}$ , where  $[k]$  refers to the part of the stiffness matrix corresponding to degrees of freedom 1, 2. The remaining terms of  $\{p^{er}\}$ , corresponding to the degrees of freedom 3, 4 are obtained by using the equilibrium conditions.

The residual force vector,  $\{p^{er}\}$  of the elements is assembled to form the residual force vector,  $\{P^{er}\}$  of the RC member.  $\{P^{er}\}$  should be within some permissible limit (Ghali *et al.* 2002) for the iterative process to terminate, typically

$$\left[ \{P^{er}\}^T \{P^{er}\} \right]^{1/2} \leq \lambda \left[ \{P^o\}^T \{P^o\} \right]^{1/2} \quad (53)$$

where,  $\lambda$  = tolerance value (taken as 0.001),  $\{P^o\}$  = fixed end force vector of the uncracked element. Otherwise, a new cycle is started.

## 5. Validation

The proposed tension stiffening model (and developed procedure) has been validated with the experimental results available in literature for one-way slabs and beams and also with the finite element method (FEM) results.

### 5.1 Simply supported rectangular beams

First, in order to validate the proposed tension stiffening model (and developed procedure) for highly reinforced members under mid-span concentrated load, three simply supported beams (B36L-1, B44-1, B18-2) of rectangular cross-section are considered, for which experimental results were reported by Kalkan (2010). The percentage tensile reinforcement and other relevant data are given in Table 1. Further,  $E_s$  was taken as 200,000 N/mm<sup>2</sup>.

Mid-span deflections, for beams B36L-1, B44-1, and B18-2, from the proposed procedure, experiments (Kalkan 2010), Bischoff (2005) and ACI 318 (2005) are compared in Fig. 7 under increasing concentrated load,  $W$ . Close agreement between the results from the proposed procedure, experiments (Kalkan 2010), Bischoff (2005) and ACI 318 (2005) is observed.

Table 1 Properties of simply supported beams and one-way slabs

Beams/Slabs	Properties						
	$L$ (mm)	$B_f = B_w$ (mm)	$D$ (mm)	$d_b$ (mm)	$\rho$ (%)	$E_c$ (N/mm <sup>2</sup> )	$f_t$ (N/mm <sup>2</sup> )
B36L-1	11890	76	914	139	3.46	29650	2.62
B44-1	11890	76	1118	165	2.81	30700	3.16
B18-2	3660	38	457	68	4.06	34450	4.56
S1	3500	850	110	18	0.18	26800	3.39
S2	3500	850	110	19	0.29	26800	3.39
S3	3500	850	110	20	0.46	26800	3.39
S8	3500	850	110	21	0.45	30700	4.16

### 5.2 Simply supported rectangular one-way slabs

Further, in order to ensure the applicability of the proposed tension stiffening model (and developed procedure) for lightly reinforced members under mid-span concentrated load, four simply supported one-way slabs (S1, S2, S3, S8) of rectangular cross-section are considered, for which experimental results were reported by Gilbert (2006). The percentage tensile reinforcement and other relevant data are given in Table 1. Further,  $E_s$  was taken as 200,000 N/mm<sup>2</sup>.

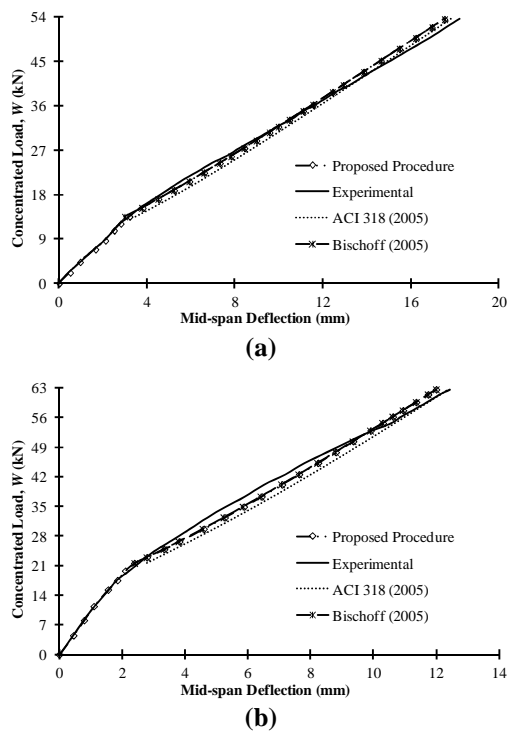


Fig. 7 Comparison of mid-span deflections in beams: (a) B36L-1; (b) B44-1; and (c) B18-2

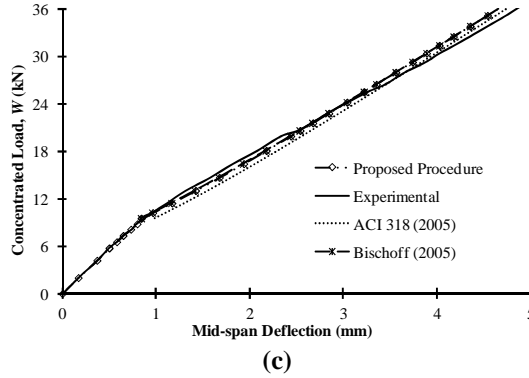


Fig. 7 Continued

Mid-span deflections, for slabs S1, S2, S3, and S8, from the proposed procedure, experiments (Gilbert 2006), ACI 318 (2005) and Bischoff (2005) are compared in Fig. 8 under increasing concentrated load,  $W$ . Close agreement between the results from the proposed procedure, experiments (Gilbert 2006) and Bischoff (2005) is observed, whereas, significant error is observed in results from ACI 318 (2005).

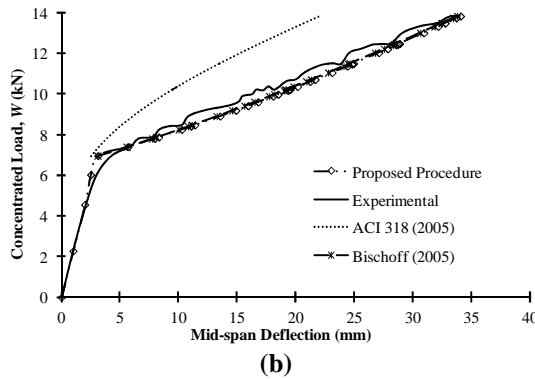
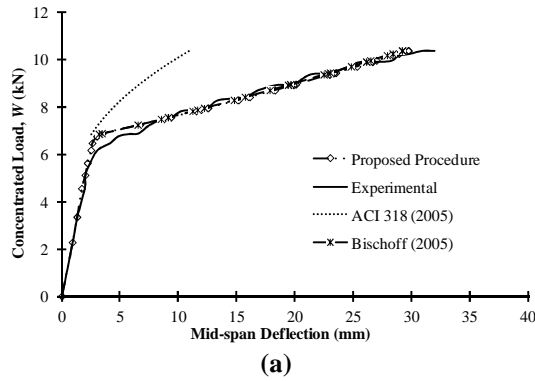


Fig. 8 Comparison of mid-span deflections in slabs (a) S1; (b) S2; (c) S3; and (d) S8



Table 2 Continued

$d_t$ (mm)	-	39.63	39.63	-	-	-
$d_b$ (mm)	45.98	45.98	45.98	58.94	55.64	45.98
$A_{st}$ (mm <sup>2</sup> )	-	200.09	400.19	-	-	-
$A_{sb}$ (mm <sup>2</sup> )	400.19	400.19	400.19	774.56	400.19	400.19
$f'_c$ (N/mm <sup>2</sup> )	25.37	26.77	24.27	25.37	29.36	29.36
$E_c$ (N/mm <sup>2</sup> )	25286	25975	24732	25286	27202	27202
$E_s$ (N/mm <sup>2</sup> )	205000	205000	205000	205000	205000	205000
$w$ (N/mm)	6.42	6.44	6.41	11.73	12.29	3.79
$f_t$ (N/mm <sup>2</sup> )	2.78	2.66	2.73	2.78	3.06	3.06
$L$ (mm)	6098	6098	6098	6098	4268	6098

Table 3 Comparison of mid-span deflections

Mid-span deflections	Beams					
	A-1	B-1	C-1	D-1	E-1	F-1
$d_{PP}$ (mm)	28.35	28.25	28.03	31.04	13.60	50.57
$d_{EXP}$ (mm)	34.04	31.50	30.23	32.23	12.96	55.89

#### 5.4 Continuous rectangular beams

The results from proposed tension stiffening model (and developed procedure), have been compared with the experimental results (deflections) reported by Washa and Fluck (1956) for nine sets of two span continuous beams: X1,X4; X2,X5; X3,X6; Y1,Y4; Y2,Y5; Y3,Y6; Z1,Z4; Z2,Z5; Z3,Z6 subjected to uniformly distributed loads,  $w$  (see Fig. 9 and Table 4). Additionally,  $E_s=206,843$  N/mm<sup>2</sup> and  $f_t=0.623\sqrt{f'_c}$  N/mm<sup>2</sup> (ACI 318 2005) were taken. Two beams in a set are identical.

Table 4 Properties of two span continuous beams

Beam	$B_w \times D$ (mm×mm)	$E_c$ (N/mm <sup>2</sup> )	$f'_c$ (N/mm <sup>2</sup> )	$w$ (kN/m)	$L_1=L_2$ (m)	$d_t = d_b$ (mm)	EF		AE, FC	
							$A_{sb}$	$A_{st}$	$A_{sb}$	$A_{st}$
							(mm <sup>2</sup> )		(mm <sup>2</sup> )	
X1,X4	152.4×203.2	23235	25.34	2.770	6.10	40	600	684	400	400
X2,X5	152.4×203.2	23235	25.34	2.770	6.10	40	600	684	400	200
X3,X6	152.4×203.2	23235	25.34	2.770	6.10	40	600	684	400	-
Y1,Y4	304.8×127.0	23270	27.51	2.131	6.34	24	1000	1000	516	516
Y2,Y5	304.8×127.0	23270	27.51	2.131	6.34	24	1000	1000	516	258
Y3,Y6	304.8×127.0	23270	27.51	2.131	6.34	24	1000	1000	516	-
Z1,Z4	304.8×76.2	22994	25.92	0.993	5.33	16	645	516	284	284
Z2,Z5	304.8×76.2	22994	25.92	0.993	5.33	16	645	516	284	142
Z3,Z6	304.8×76.2	22994	25.92	0.993	5.33	16	645	516	284	-

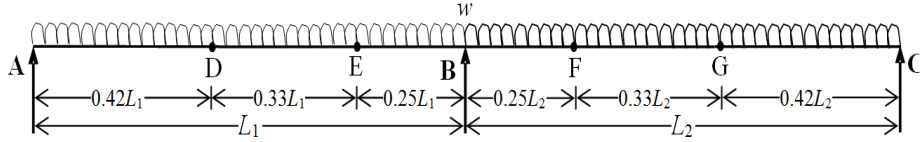


Fig. 9 Two span continuous beam

For FEM results, modeling has been done in the ABAQUS (2011) software (Thevendran *et al.* 2000, Baskar *et al.* 2002, Shanmugam and Baskar 2003, Ramnavas *et al.* 2015). The beam is modelled using B21 elements (2-node linear Timoshenko beam element in plane). Under service load, the stress-strain relationship of concrete is assumed to be linear in compression. Concrete is considered as an elastic material in tension before cracking and softening behavior is assumed linearly after cracking (see Fig. 10). Tension stiffening is defined in the model using post-failure stress-strain data. In order to define the smeared crack model, the absolute value of the ratio of uniaxial tensile stress at failure to the uniaxial compressive stress at failure is obtained using concrete properties. In view of moderate tensile reinforcements, the plastic strain ( $\varepsilon_u - \varepsilon_t$ ) is taken as 0.0009. Further, at service load, the stress in reinforcement is assumed to be in the linear range.

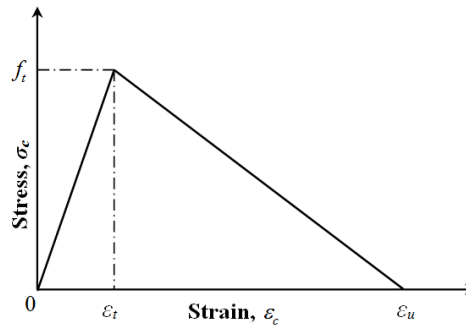


Fig. 10 Tension stiffening model

Table 5 Comparison of results from the proposed procedure, experiments and FEM

Beam	Deflection at D (mm)		
	Proposed Procedure	Experimental Washa and Fluck (1956)	FEM ABAQUS (2011)
X1,X4	14.5226	14.2240	14.4608
X2,X5	14.7747	14.4780	14.6436
X3,X6	15.0774	15.7480	15.0278
Y1,Y4	23.3311	22.6060	22.1316
Y2,Y5	23.9296	23.6220	22.9430
Y3,Y6	24.6651	25.4000	23.9422
Z1,Z4	28.5579	26.4160	26.8351
Z2,Z5	29.0868	28.7020	27.6168
Z3,Z6	29.7183	30.4800	27.6548

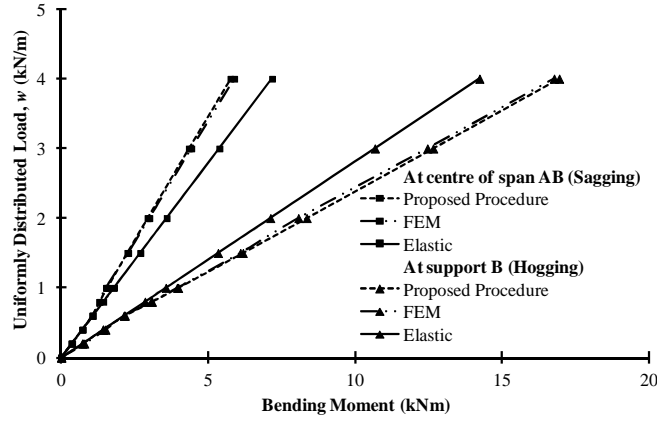


Fig. 11 Comparison of bending moments of beam Z1,Z4

The experimental results (deflections) and those obtained from the proposed procedure are shown in Table 5 along with the results obtained by FEM. In FEM, convergence was achieved with 16 elements in a span. Close agreement between the results from the procedure, experiments and FEM is observed. Further, bending moment at the centre of span AB and at support B for the beam Z1,Z4 obtained from the proposed procedure and FEM are shown in Fig. 11. Also shown, for comparison, are the bending moments obtained neglecting cracking. Close agreement between the results obtained from the proposed procedure and FEM is observed.

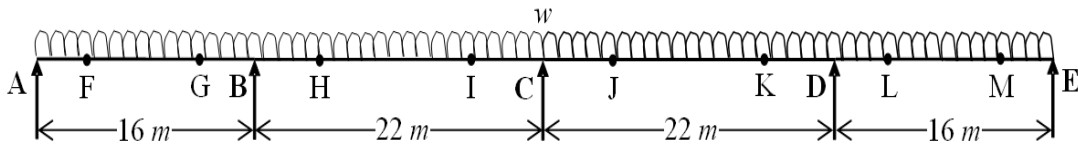


Fig. 12 Four span continuous bridge VB with T cross-section

### 5.5 Continuous T bridge

Further, in order to validate the proposed tension stiffening model (and developed procedure) for a four span continuous bridge with T cross-section VB, results (deflections) from the proposed procedure have been compared with FEM results (see Fig. 12). The cross-section dimensions of flange ( $B_f \times D_f$ ) and web ( $B_w \times D_w$ ) are  $1000 \times 125$  mm and  $700 \times 1400$  mm respectively. The other properties are:  $E_c = 31,176$  N/mm<sup>2</sup>,  $E_s = 206,000$  N/mm<sup>2</sup>,  $f_t = 4.13$  N/mm<sup>2</sup>. The areas of reinforcements are shown in Table 6. The effective concrete covers  $d_t = d_b = 75$  mm have been taken. Results from the proposed procedure and FEM have been obtained for varying magnitude of uniformly distributed loads,  $w$ . In FEM, convergence was achieved with 32 elements in a span. Fig. 13 presents comparison of mid-deflections at the center of span AB and BC and again, close agreement is observed.

Table 6 Reinforcement detailing data of bridge VB

Segment (Fig. 12)	AF, ME	FG, LM	GB, DL	BH, IC, CJ, KD	HI, JK
Length (m)	4.00	8.00	4.00	5.50	11.00
$A_{st}$ (mm <sup>2</sup> )	5027	4825	12566	12566	4825
$A_{sb}$ (mm <sup>2</sup> )	5027	10178	4825	4825	10178

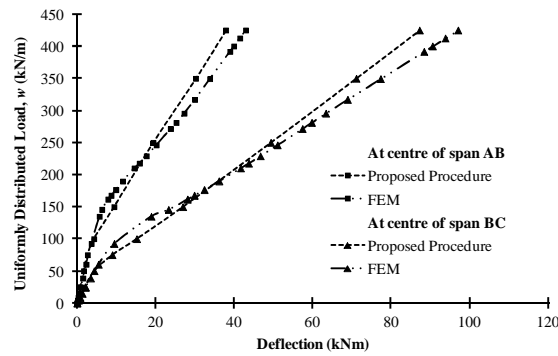


Fig. 13 Comparison of mid-span deflections of bridge VB

Table 7 Half band-width,  $p$  and total number of DOF,  $q$  for beam Z1,Z4 and bridge VB

Beam/Bridge	Half band width ( $p$ )		Number of elements in each span		Total number of DOF ( $q$ )	
	PP <sup>#</sup>	FEM	PP <sup>#</sup>	FEM	PP <sup>#</sup>	FEM
Z1,Z4	4	4	1	16	6	66
VB	4	4	1	32	10	258

<sup>#</sup>PP = Proposed procedure

## 6. Computational efficiency

In order to compare the computational effort required in the proposed procedure and FEM, half band-width,  $p$ , and the total number of degree of freedom (DOF),  $q$  are presented in Table 7 for beam Z1,Z4 and bridge VB. The numbers of elements indicated for FEM are those that result in convergence of deflection within 1%. Noting that the major portion of the computational effort required in the procedure in an iteration is proportional to  $qp^2/2$ , the ratio of computational effort required in the proposed procedure to that in FEM, in an iteration is about 1/11 and 1/26 for beams Z1,Z4 and bridge VB respectively. Further noting that the number of iterations required in the proposed procedure is about 1/4 of that required in the FEM for the beam and bridge, the total computational effort required in the proposed procedure is about 1/44 and 1/103 of that required in FEM for beam Z1,Z4 and bridge VB respectively.

## 7. Conclusions

A tension-stiffening model has been proposed for computationally efficient nonlinear analysis

of RC flexural members (one-way slabs, beams and bridges) subjected to service load. The proposed model has been further embedded in a typical cracked span length beam element. The element is visualized to consist of at the most five zones (cracked or uncracked). Closed form expressions for flexibility and stiffness coefficients and end displacements have been obtained for the cracked span length beam element. Further, for use in everyday design, a hybrid analytical-numerical procedure has been developed for nonlinear analysis of RC flexural members using the proposed tension-stiffening model. The procedure yields deflections as well as redistributed bending moments. The results obtained from the proposed tension stiffening model (and developed procedure) are shown to be in reasonable agreement with the experimental and FEM results for entire practical range of tensile reinforcement in flexural members. Use of the proposed model (and developed procedure), for the analysis of RC multi-span continuous bridges incorporating cracking, can save a considerable amount of computational time as the proposed procedure requires a computational effort, that is a small fraction of that required in the FEM.

The proposed procedure is being further developed for time-effects (creep and shrinkage) in RC members considering progressive cracking where again a huge reduction in computational effort would result.

## References

- ABAQUS (2011), ABAQUS standard user's manuals, Version 6.11, Hibbit, Karlsson and Sorensen, Inc., Pawtucket, RI, USA.
- ACI 318 (2005), Building code requirements for structural concrete, American Concrete Institute (ACI) Committee 318, Farmington Hills, MI, USA.
- Balakrishnan, S. and Murray, D.W. (1988), "Concrete constitutive model for NLFE analysis of structures", *J. Struct. Eng.*, **114**(7), 1449-1466.
- Baskar, K., Shanmugam, N.E. and Thevendran, V. (2002), "Finite-element analysis of steel-concrete composite plate girder", *J. Struct. Eng.*, **128**(9), 1158-1168.
- Bischoff, P.H. (2005), "Reevaluation of deflection prediction for concrete beams reinforced with steel and fiber reinforced polymer bars", *J. Struct. Eng.*, **131**(5), 752-767.
- Borosnyói, A. and Balázs, G.L. (2005), "Models for flexural cracking in concrete: the state of the art", *Struct. Concrete*, **6**(2), 53-62.
- CEN-Eurocode 2 (2004), Design of concrete structures-Part 1-1: General rules and rules for buildings, European Standard BS EN 1992-1-1:2004, Brussels.
- Cosenza, E. (1990), "Finite element analysis of reinforced concrete elements in a cracked state", *Comput. Struct.*, **36**(1), 71-79.
- Dai, J.G., Ueda, T., Sato, Y. and Nagai, K. (2012), "Modeling of tension stiffening behavior in FRP-strengthened RC members based on rigid body spring networks", *Comput. Aid. Civil Infrastruct. Eng.*, **27**(6), 406-418.
- Ghali, A. (1993), "Deflection of reinforced concrete members: A critical review", *ACI Struct. J.*, **90**(4), 364-373.
- Ghali, A., Favre, R. and Elbadry, M. (2002), *Concrete structures: Stresses and deformations*, 3rd Edition, E and Spon, London, UK.
- Ghali, A., Neville, A.M. and Brown, T.G. (2003), *Structural analysis: A unified classical and matrix approach*, 5th Edition, Spon press, New York, USA.
- Gilbert, R.I. (2006), "Discussion of 'Reevaluation of deflection prediction for concrete beams reinforced with steel and fiber reinforced polymer bars' by Bischoff, P.H.", *J. Struct. Eng.*, **132**(8), 1328-1330.
- Kalkan, İ. (2010), "Deflection prediction for reinforced concrete beams through different effective moment of inertia expressions", *Int. J. Eng. Res. Dev.*, **2**(1), 72-80.

- Lackner, R. and Mang, H.A. (2003), "Scale transition in steel-concrete interaction. I: Model", *J. Eng. Mech.*, **129**(4), 393-402.
- Massicote, B., Elwi, A.E. and MacGregor, J.G. (1990), "Tension-stiffening model for planar reinforced concrete members", *J. Struct. Eng.*, **116**(11), 3039-3058.
- Ning, F., Mickleborough, N.C. and Chan, C.M. (1999), "The effective stiffness of reinforced concrete flexural members under service load conditions", *Aust. J. Struct. Eng.*, **2**, 135-144.
- Park, R. and Paulay, T. (1975), *Reinforced concrete structures*, John Wiley and Sons Inc., Canada.
- Parrotta, J.E., Peiretti, H.C., Gribniak, V. and Caldentey, A.P. (2014), "Investigating deformations of RC beams: experimental and analytical study", *Comput. Concrete*, **13**(6), 799-827.
- Patel, K.A., Bhardwaj, A., Chaudhary, S. and Nagpal, A.K. (2015), "Explicit expression for effective moment of inertia of RC Beams", *Lat. Am. J. Solid Struct.*, **12**(3), 542-560.
- Patel, K.A., Chaudhary, S. and Nagpal, A.K. (2014), "Analytical-numerical procedure incorporating cracking in RC beams", *Eng. Comput.*, **31**(5), 986-1010.
- Ramnavas, M.P., Patel, K.A., Chaudhary, S. and Nagpal, A.K. (2015), "Cracked span length beam element for service load analysis of steel concrete composite bridges", *Comput. Struct.*, **157**, 201-208.
- Ruiz, M.F., Muttoni, A. and Gambarova, P.G. (2007), "Analytical modeling of the pre- and postyield behavior of bond in reinforced concrete", *J. Struct. Eng.*, **133**(10), 1364-1372.
- Sahamitmongkol, R. and Kishi, T. (2011), "Tension stiffening effect and bonding characteristics of chemically prestressed concrete under tension", *Mater. Struct.*, **44**(2), 455-474.
- Salys, D., Kaklauskas, G. and Gribniak, V. (2009), "Modelling deformation behaviour of RC beams attributing tension-stiffening to tensile reinforcement", *Eng. Struct. Tech.*, **1**(3), 141-147.
- Scanlon, A., Cagley Orsak, D.R. and Buettner, D.R. (2001), "ACI code requirements for deflection control: A critical review", *ACI S.P.*, **203**, 1-14.
- Shanmugam, N.E. and Baskar, K. (2003), "Steel-concrete composite plate girders subject to shear loading", *J. Struct. Eng.*, **129**(9), 1230-1242.
- Shayanfar, M.A. and Safiey, A. (2008), "A new approach for nonlinear finite element analysis of reinforced concrete structures with corroded reinforcements", *Comput. Concrete*, **5**(2), 155-174.
- Smadi, M.M. and Belakhdar, K.A. (2007), "Nonlinear finite element analysis of high strength concrete slabs", *Comput. Concrete*, **4**(3), 187-206.
- Stramandinoli, R.S.B. and Rovere, H.L.L. (2008), "An efficient tension-stiffening model for nonlinear analysis of reinforced concrete members", *Eng. Struct.*, **30**(7), 2069-2080.
- Thevendran, V., Shanmugam, N.E., Chen, S. and Richard Liew J.Y. (2000), "Experimental study on steel-concrete composite beams curved in plan", *Eng. Struct.*, **22**(8), 877-889.
- Vollum, R.L., Afshar, N. and Izzuddin, B.A. (2008), "Modelling short-term tension stiffening in tension members", *Mag. Concrete Res.*, **60**(4), 291-300.
- Washa, G.W. and Fluck, P.G. (1956), "Plastic flow (creep\*) of reinforced concrete continuous beams", *ACI Struct. J.*, **52**(1), 549-561.
- Yu, W.W. and Winter, G. (1960), "Instantaneous and long-time deflections of reinforced concrete beams under working loads", *ACI J.*, **57**(1), 29-50.

CC

## Notations

- $A, B, I$  : area, first moment of area, and second moment of area respectively;
- $A_{st}, A_{sb}$  : area of top, and bottom reinforcements respectively;
- $A_v, f$  : shearing steel area, and shear coefficient respectively;

- $B, D, d$  : width, total depth, and effective depth of section respectively;  
 $\{d^{er}\}, \{d^*\}$  : error or difference in displacement vector, and revised displacement vector respectively;  
 $d_m, L$  : mid-span deflection, and span length respectively;  
 $d_t, d_b$  : effective concrete cover at top, and bottom respectively;  
 $E, f_c'$  : modulus of elasticity, and cylinder compressive strength of concrete at 28 days respectively;  
 $f_{ij}, k_{ij}, [k]$  : flexibility, stiffness coefficients, and stiffness matrix of a skeletal member respectively;  
 $f_t, G, \mu$  : tensile strength, shear modulus, and Poisson's ratio of concrete respectively;  
 $|f|$  : determinant of flexibility matrix,  $[f]$ ;  
 $K, \nu_v$  : shearing rigidity, and shearing steel content respectively;  
 $L_i$  : length of the typical zone (cracked or uncracked);  
 $L_{i,cr}$  : length of the cracked zone;  
 $M, N, R$  : moment, axial force, and shear force respectively;  
 $M_{cr}, n$  : cracking moment, and modular ratio respectively;  
 $\{P^0\}$  : fixed end force vector for uncracked beam;  
 $\{P^{er}\}, \{p\}$  : residual force vector, and revised force vector respectively;  
 $p, q$  : half band width, and total number of DOF respectively;  
 $s, \theta, \lambda$  : spacing of reinforcements, end rotation, and tolerance value respectively;  
 $W, w$  : concentrated, and uniformly distributed loads respectively;  
 $x'$  : distance of cross-section from C in a typical zone;  
 $\xi, \eta$  : average interpolation coefficients;  
 $\kappa$  : coefficient representing influence of duration of application or repetition of loading on interpolation coefficient;  
 $\rho, \varepsilon, \sigma$  : curvature, strain, and stress respectively;  
 $\varepsilon_t, \varepsilon_u$  : cracking strain, and maximum tensile strain of concrete respectively; and  
 $\varepsilon_y$  : strain at a distance  $y$  from the reference axis.
- Subscript**
- $A, B$  : ends A and B of a cracked span length beam element respectively;  
 $c, s$  : concrete, and steel respectively;  
 $cr, un, ts$  : cracked state, uncracked state, and tension stiffening respectively;  
 $f, w$  : flange, and web respectively;  
 $i$  :  $i^{th}$  zone;  
 $n, r$  : net, and relative respectively; and  
 $y$  : distance from the reference axis.
- Superscript**
- $C, D, E$  : locations in a typical zone; and  
 $m, n$  : moment, and axial force respectively.